# The *Arabidopsis lue1* mutant defines a katanin p60 ortholog involved in hormonal control of microtubule orientation during cell growth

**Thomas Bouquin, Ole Mattsson, Henrik Næsted, Randy Foster and John Mundy***

Institute of Molecular Biology, Department of Plant Physiology, Øster Farimagsgade 2A, 1353K Copenhagen, Denmark

*Author for correspondence (e-mail: mundy@biobase.dk)

*Accepted 15 November 2002*
*Journal of Cell Science 116, 791-801 © 2003 The Company of Biologists Ltd*
*doi:10.1242/jcs.00274*

## Summary

**The *lue1* mutant was previously isolated in a bio-imaging screen for *Arabidopsis* mutants exhibiting inappropriate regulation of an *AtGA20ox1* promoter-luciferase reporter fusion. Here we show that *lue1* is allelic to *fra2*, *bot1* and *erh3*, and encodes a truncated katanin-like microtubule-severing protein (*At*KSS). Complementation of *lue1* with the wild-type *AtKSS* gene restored both wild-type stature and luciferase reporter levels. Hormonal responses of *lue1* to ethylene and gibberellins revealed inappropriate cortical microtubule reorientation during cell growth. Moreover, a fusion between the AtKSS protein and GFP decorated cortical microtubules. A yeast two-hybrid screen with AtKSS as the bait identified proteins related to those involved in microtubule processing, including a katanin p80 subunit and a kinesin ortholog. These results indicate that *AtKSS* is involved in microtubule dynamics in response to plant hormones.**

Key words: Gibberellins, Katanin, Kinesin, *lue1*, Microtubules

## Introduction

The shape and growth orientation of plant cells are primarily controlled by cellulose microfibrils (CMF) of the cell wall and by microtubules (MT) of the cytoskeleton (reviewed in Kost et al., 1999; Azimzadeh et al., 2001; Wasteneys, 2002). The molecular mechanisms involved are being analyzed via the characterization of mutants with altered cell wall and MT organization. For example, both *Arabidopsis rsw1* and *kor* mutants exhibit altered cellulose microfibril (CMF) organization and composition, and *RSW1* and *KOR*, respectively, encode a cellulose synthase subunit (Arioli et al., 1998) and a membrane-bound endo (1-4)-β-D glucanase (Nicol et al., 1998; Zuo et al., 2000). More recently, the *mor1* mutant was shown to be defective in MT organization. *MOR1* encodes a new class of plant MT-interacting proteins (Whittington et al., 2001). Three other *Arabidopsis* allelic mutants, *bot1, fra2* and *erh3*, exhibit disorganized CMT, leading to isotropic cell growth, inflorescence stem fragility and ectopic root hair (Bichet et al., 2001; Burk et al., 2001; Webb et al., 2002). These loci encode a 60 kDa microtubule-associated ATPase katanin ortholog designated *At*KSS (McClinton et al., 2001). In animal cells, katanin is a heterodimer consisting of the 60 kDa ATPase that harbors MT-severing activity and an 80 kDa subunit that targets the heterodimer to centrosomes (Hartman et al., 1998; McNally et al., 2000). The in vitro MT-severing activity of *At*KSS has recently been reported (Stoppin-Melllet et al., 2002).

Plant MT organization is under the control of external stimuli and endogenous signals, including hormones (reviewed by Shibaoka, 1994). For example, auxin, gibberellin (GA) and brassinosteroid treatments lead to a modification of cortical MT (CMT) orientation into a transverse array (Ishida and Katsumi, 1992; Baluska et al., 1993; Zandomeni and Schopfer, 1993). By contrast, ethylene (ET) and abscisic acid, an antagonist of GA, promote an oblique orientation. In the GA-deficient maize *d5* dwarf, CMTs exhibit an oblique orientation that can be restored to the wild-type transverse orientation upon GA application, which results in normal growth (Baluska et al., 1993). Moreover, the use of a GA biosynthesis inhibitor leads to a CMT misorientation in wild-type root cells that is similar to that in *d5*. More recent work has confirmed the role of GA in reorienting the CMT network in root and leaf cells (Inada and Simmen, 2000; Wenzel et al., 2000). Despite these observations, molecular data linking GA responses to CMT organization remain sparse.

Two major genes affecting responses to GA have been identified in phenotypic screens for growth mutants. Dominant mutations of *GAI/RGA*, which encode GRAS proteins proposed to function as the metazoan STAT transcription factors (Richards et al., 2000), result in semi-dwarfism, an important agronomic trait. Recessive mutations in *SPY*, which encodes an *O*-linked *N*-acetylglucosamine transferase [OGT (Thornton et al., 1999)], result in elongated plants with a constitutive GA-response phenotype. In attempts to identify additional genes involved in GA responses, we developed a fusion genetic approach to identify trans-acting mutations affecting the expression of transgenes composed of the firefly luciferase reporter under the control of the promoter of *AtGA20ox1*, which encodes the biosynthetic GA20-oxidase (Meier et al., 2001). The *AtGA20ox1* promoter was used because expression from it is regulated through negative feedback by active product GAs; therefore, cis-elements in the promoter may be targets for GA signaling pathways. This screen identified the recessive, semi-

dwarf *lue1* mutant. *Lue1* exhibited constitutive, high levels of LUC reporter and *AtGA20ox1*mRNA, as well as inappropriate feedback regulation of the endogenous *AtGA20ox1*and *At3ox1* biosynthetic genes by GA. Additionally, wild-type stature could not be rescued by GA applications. These results indicated that the sensitivity of *lue1* to GA was altered at the levels of both GA biosynthetic feedback and vegetative cellular responses.

We show here that *lue1* is allelic to *fra2* and *bot1*. Complementation of *lue1* with the wild-type *AtKSS* gene restored normal stature and luciferase reporter levels. Treatments of *lue1* with ET and GA revealed inappropriate hormonal responses related to cell growth. A reporter fusion between *At*KSS and GFP revealed that *At*KSS decorates the CMT in a punctate pattern. Moreover, a yeast two-hybrid screen performed with *At*KSS as the bait identified proteins related to those involved in MT growth and processing, including a katanin p80 and a large protein containing a kinesin-like domain. Potential links between GA signalling and MT organization are discussed.

## Materials and Methods

### Plant material and treatments

Seeds were surface-sterilized, plated on MS medium supplemented with 7% agar, 1% sucrose and appropriate hormones, then vernalized in the dark at 4°C for 4 days. For gibberellin treatments, 1-week-old seedlings were transferred to soil and grown under long-day conditions. Plants were sprayed twice a week with 10 μM $GA_3$ or 10 μM $GA_4$ (Sigma) until bolting. *Lue1* mutant sensitivity to ET in the dark was investigated by plating wild-type and *lue1* seeds on MS medium supplemented with 7% agar, 1% sucrose with or without 50 μM ACC (Sigma); thereafter plates were incubated vertically (to facilitate root measurements) at 21°C in the dark. Hypocotyl width was measured in the region exhibiting maximum diameter. *Lue1* sensitivity to ET under light conditions was performed as described previously (Smalle et al., 1997), except that 50 μM ACC (Sigma) was used instead of gaseous ET. The *ga1-1* mutant was obtained from the Nottingham *Arabidopsis* Stock Center. N.-H. Chua, Rockefeller University, kindly provided plants expressing the GFP-talin and microtubule-associated protein 4 (MP4)-GFP reporters that, respectively, decorate actin (Kost et al., 1998) and MT (Mathur and Chua, 2000). The *lue1* mutant was crossed with the GFP-talin and GFP-MAP4 lines. $F_2$ segregating seedlings were then scored for WT or *lue1* phenotype before being subjected to confocal laser-scanning microscopy.

### AtKSS gene cloning and lue1 complementation

The *AtKSS* gene was PCR-amplified with template DNA from BAC F5I6 and linker-primers 5′AC*AAGCTT*GTTGGTCCTGGCCAG-TCAGAC and 5′CTT*AGATCT*ACATCCGGAGTCCTCCTTAGC. Products were digested with *Hin*dIII and *Bgl*II and subcloned in the *Hin*dIII and *Bam*HI sites of the *pCambia3300* vector (Cambia, Canberra) to produce *C3300-AtKSS*. This construct was introduced into *Agrobacterium tumefaciens* (PGV3101) by electroporation, which was used to transform the *lue1* mutant by vacuum infiltration (Bechtold and Pelletier, 1998). $T_1$ generation seedlings were selected in soil for phosphinothricin resistance expressed from the *pCambia3300* T-DNA by spraying seedlings every 3 days with 10 mg/l Bastamycin (AgrEvo, Denmark).

### CaMV35S-AtKSS-GFP-GUS reporter

*AtKSS* wild-type genomic DNA was PCR-amplified by RT-PCR using linker-primers 5′*AGATCT*GGGAAGTAGTAATTCGTTAGCGGGTC and 5′*AGATCT*CCAAACTCAGAGAGCCACTTCTCGTG. PCR was performed for 30 cycles using Vent DNA polymerase (NEB) and *Arabidopsis* Col0 genomic DNA as the template. The product was digested with *Bgl*II and cloned into the same site of pCAMBIA1304 (Cambia, Canberra) to produce the *C1304-AtKSS-GFP-GUS* fusion reporter. The *AtKSS* sequence and correct fusion open reading frame were confirmed by sequencing. This construct was transformed via the *A. tumefaciens* strain PGV3101 into *lue1* and *Arabidopsis* Col ecotype by vacuum infiltration. $T_1$ seedlings were selected for hygromycin resistance, carried on the pCAMBIA1304 T-DNA, on MS plates with 50 mg/l hygromycin B. Homozygous single insertion lines were selected from the $T_3$ generation and approximately 20 lines analyzed further.

### Reporter assays

Equipment and protocols for LUC bioluminescence imaging were described previously (Meier et al., 2001). GFP was visualized using a Zeiss LSM 510 laser-scanning microscope applying the 488 nm line of the argon laser and the corresponding dichroic mirror and a 505-530 nm band-pass filter. For reference, chlorophyll fluorescence and a Nomarski image were recorded simultaneously.

### RNA analysis

Total RNA (10 μg) extracted with the RNAgent kit (Promega) was fractionated on standard formaldehyde gels and blotted onto Hybond-N+ membranes (Amersham). *AtKSS* mRNA levels were investigated by hybridization with a ribonucleic [$^{32}$P]CTP antisense probe synthesized with T7 RNA polymerase (Ribokit, Promega) from a full-length cDNA cloned in the *pGEM-Teasy* vector (Promega). *AtKSS* primers for cDNA amplification were 5′GTTAGCGGGTCTACAA-GACCAC and 5′ACTCAGAGAGCCACTTCTCGTG. Hybridization and washing conditions were performed as recommended by the manufacturer.

### Analysis of CMF orientation by polarizing microscopy

For polarizing microscopy, 5 mm segments from the lower part of the flowering stem were fixed in buffered 4% formaldehyde, embedded in paraffin wax and sectioned longitudinally at 8 μm. Positions of maximum extinction closest to the polarizing plane of the analyzer were determined visually by rotating the stage of the polarizing microscope (Frey-Wyssling, 1959). The angular absolute values of the difference between these positions and those of the long cell axis parallel to the analyzer plane were determined. The distinction between extinction parallel to the analyzer plane and to the polarizer plane was made by insertion of a red first order compensator (sensitive tint plate).

### AtKSS protein interaction analyses

The full-length *AtKSS* cDNA bait was amplified by RT-PCR with linker-primers AAA1-2hyb-F (GAG*GAATTC*GTGGGAAGTAGTA-ATTCGTTAGCG) and AAA1-2hyb-R (GGG*AGATCT*TAAGCAGA-TCCAAACTCAGAGAGC). The product was digested with *Bam*HI and *Bgl*II and subcloned in the *Bam*HI site of *pGBKT7* (Clontech Matchmaker System III) to produce *pGBKT7-AtKSS*, which was introduced into yeast strain PJ69A-4A. This bait strain was transformed with a cDNA library from mature leaf mRNA in vector *pGAD10* (Clontech, FL4000AB). The yeast two-hybrid screen was performed according to the manufacturer's instructions for prototrophic growth on medium lacking tryptophan (TRP), leucine (LEU), histidine (HIS) and adenine (ADE) for 4 days at 30°C. A total of $15\times10^6$ transformants were screened to yield some 1000 positive clones. These clones were assayed for β-galactosidase activity, which eliminated roughly 50% of the clones. DNA was extracted from the

remainder and approximately 100 clones were used as PCR templates with *pGAD10* primers (Clontech, 9103-1) to size inserts and for sequencing. Sequencing allowed us to discard clones containing frame shifts between the GAL4-binding domain (GAL4-BD) and the prey clones or clones inserted in the reverse orientation. One clone from each of the remaining prey insert groups was mobilized in *E. coli* and re-sequenced. To confirm interactions, bait and prey plasmids were individually co-transformed into PJ69A-4A and re-evaluated for prototrophic growth and β-galactosidase activity. To confirm AtKSS interactions, prey cDNAs were subcloned into the T7 RNA polymerase promoter-containing *pGAD-T7* plasmid (Clontech). Additionally, a truncated version (1.25B2) of the *KTN P80.1* clone 1.25 was constructed by restriction digestion with *Bgl*II and subsequent cloning into the *Bam*HI site of *pGADT7*. Correct orientation of the insert and frame were assessed by restriction digestion and sequencing. All pGADT7-based constructs were confirmed for interaction with AtKSS in directed yeast two-hybrid assays by co-transformation of the yeast PJ69A-4A with *pGBKT7-AtKSS*. Additionally, an empty *pGBKT7* (i.e. without the *AtKSS* fusion) was co-transformed with the *pGADT7*-based vectors to confirm that both β-galactosidase activity and prototrophic growth require AtKSS-prey proteins interaction. To further confirm AtKSS interactions, bait and prey proteins were synthesized by in vitro transcription/translation using the T7-RNA-polymerase-based TnT kit (Promega, #L4610) in the presence of $^{35}$S-methionine and co-immunoprecipitated with protein-G-coupled Dynabeads (Dynal Biotech, #100.03/04) according to the manufacturer's instructions. An in-vitro-translated c-Myc-tagged lamin C (pGBKT7-Lam, Clontech) was used as a control in co-immunoprecipitation assays.

### Genetic analyses

*Lue1* was previously mapped with SSLP markers (Bell and Ecker, 1994) to the bottom of chromosome 1, south of marker nga692 (Meier et al., 2001). New SSLP markers were generated by comparison with Col0 and Ler ecotype DNA sequences available from Cereon Genomics (http://godot.ncgr.org/cereon/). The following primer combinations were used: F18B13-2-F (5′TTAATTATGGTTTCA-TGATCATGG) and F18B13-2-R (5′CTTTCCTTACACATCTTTC-CTGC) from BAC F18B13; F23A5-2-F (5′CTCGAGATCTAGA-CATGGAGC) and F23A5-2-R (5′GTCTAGGTTCAACAATGCTGC) from BAC F23A5; F9K20-1-F (5′TCCTCCGCTTCCGATTGGTC) and F29K20-1-R (5′GGTACCGTCACGTTCGCCGT) from BAC F29K20; T8K14-1-F (5′CAATGCGCTCTGAATCTCTGAC) and T8K14-1-R (5′CCATTCACCCACTCTTGACTC) from BAC T8K14.

## Results

### A nonsense mutation in *AtKSS* is responsible for the *lue1* phenotype

We had previously mapped the *lue1* mutation to the bottom of chromosome 1, south of SSLP marker nga692 (Meier et al., 2001). To more finely map the mutation, we designed SSLP markers following a sequence comparison between the Col0 and Ler ecotypes from Cereon Genomics (http://godot.ncgr.org/cereon/). This allowed the *lue1* mutation to be located south of BAC T8K14. A search for genes putatively involved in cell elongation or GA responses in this region identified three candidates on BAC F5I6: two encoding *At3ox1* homologs, and one encoding *At*KSS (McClinton et al., 2001), a katanin p60 ortholog. Since the *lue1* phenotype is not rescued by GA application (Meier et al., 2001), GA deficiency owing to loss of function of a *At3ox1* homolog was not considered a likely cause of the dwarf stature of *lue1* mutants. Moreover, polarizing microscopy of cell walls (below) indicated an abnormal CMF orientation in *lue1*. Hence, the *At*KSS gene was a likely candidate, and it was PCR-amplified and sequenced from *lue1*. Sequencing identified a single base change in *AtKSS* producing a nonsense mutation at amino acid 394. Shortly after, the phenotype of the *fra2* mutant was shown to be the result of another loss-of-function mutation in the *AtKSS* gene (Burk et al., 2001). In addition, recombinant AtKSS has recently been shown to posses ATP-dependent, microtubule-severing activity in vitro and is therefore a p60 katanin plant ortholog (Stoppin-Mellet et al., 2002).

To confirm that loss of AtKSS function was responsible for the *lue1* mutant phenotype, the *AtKSS* gene, including 1.7 kb of 5′UTR and 1.3 kb of 3′UTR, was amplified from the Col0 ecotype and mobilized into *lue1* via the vector *C3300-AtKSS*. Fig. 1A shows that the wild-type *AtKSS* gene rescued the *lue1* dwarf phenotype, indicating that the nonsense mutation in *AtKSS* is responsible for the *lue1* phenotype. Phenotypic rescue was observed for all bastamycin-resistant $T_1$ plants. Moreover, herbicide resistance carried on the *C3300-AtKSS* construct was found to co-segregate with the wild-type phenotype in subsequent generations.

To check whether *GA5-LUC* reporter overexpression in *lue1* (Meier et al., 2001) (Fig. 1B) would be restored to wild-type levels in *lue1* plants complemented by the *C3300-AtKSS* construct, homozygous $T_3$ generation seedlings were grown on MS plates and assayed for LUC activity in vivo. Strong reporter activity was detected in *lue1* (Fig. 1C), whereas *lue1* plants carrying *C3300-AtKSS* exhibited markedly reduced LUC levels (Fig. 1D). This indicates that the *lue1* mutation in *AtKSS* is responsible for the *GA5-LUC* reporter overexpression observed in *lue1*.

### Transcriptional regulation of *AtKSS* by GA

*AtKSS* mRNA levels in *lue1* and wild-type transgenic (WT) seeds were assayed by RNA blot hybridization. This showed that *AtKSS* mRNA levels were markedly reduced in *lue1* (Fig. 1E), which suggests that the truncated ORF of the *lue1 AtKSS* allele reduces the stability of the mutant mRNA. Alternatively, AtKSS could be involved in a feed-forward regulation of its own transcription, which would be impaired in *lue1*. Since *lue1* exhibits altered regulation of both the *GA5-LUC* reporter and endogenous *AtGA20ox1* gene (Meier et al., 2001), we investigated the expression of *AtKSS* upon $GA_3$ treatment in the GA-deficient *ga1-1* mutant (Koornneef and van der Veen, 1980). This showed that *AtKSS* mRNA accumulation levels were lower in *ga1-1* than in wild-type L*er* and could be restored to wild-type levels by $GA_3$ treatment. These results indicate that GA levels modulate *AtKSS* mRNA accumulation.

### *Lue1* exhibits altered cell elongation responses to GA and ET

As *lue1* exhibits altered *AtGA20ox1* expression levels, the mutant might be affected in its responses to GA. To assess this, GA-related responses, including flowering induction and cell elongation, were compared in GA-treated WT seedlings and *lue1* seedlings grown under long-day conditions (Fig. 2). GA treatments caused both *lue1* and WT leaves to pale. Flowering could be promoted in *lue1* by application of $GA_3$ or $GA_4$, although the effect of the latter was more pronounced

(Fig. 2A). Flowering induction by GA was the same in both *lue1* and WT (Fig. 2B). Indeed, GA applications reduced FT from 40 to 30 days for both WT and *lue1* plants, indicating that the general sensitivity of *lue1* to GA was not compromised. However, the mutant exhibited decreased stem elongation in response to GA (data not shown). This apparent insensitivity of *lue1* to GA-responsive cell elongation was pronounced in leaves, such that neither blade nor petiole length was affected by GA treatment (Fig. 2C).

Preliminary germination tests revealed that hypocotyl hook formation is impaired in *lue1*. Since hooking is caused by differential cell elongation, which is regulated, at least in part, by ET, we investigated *lue1* sensitivity to ET. WT and *lue1* seeds were plated on MS supplemented with 50 μM ACC and allowed to germinate in the dark. As expected, WT seedlings exhibited a typical hook that could be increased by ACC treatment (Fig. 3A,B). By contrast, hypocotyl hook formation was impaired in *lue1* control seedlings, whereas ACC treatment did not significantly induce hooking in the mutant (Fig. 3A,B). However, other ET-induced morphological changes were unaffected in *lue1*, including hypocotyl thickening (Fig. 3C) and hypocotyl and root shortening (Fig. 3D,E).

*Lue1* sensitivity to ET was also investigated in seedlings germinated in the light, which has previously been shown to stimulate hypocotyl growth of seedlings grown on low

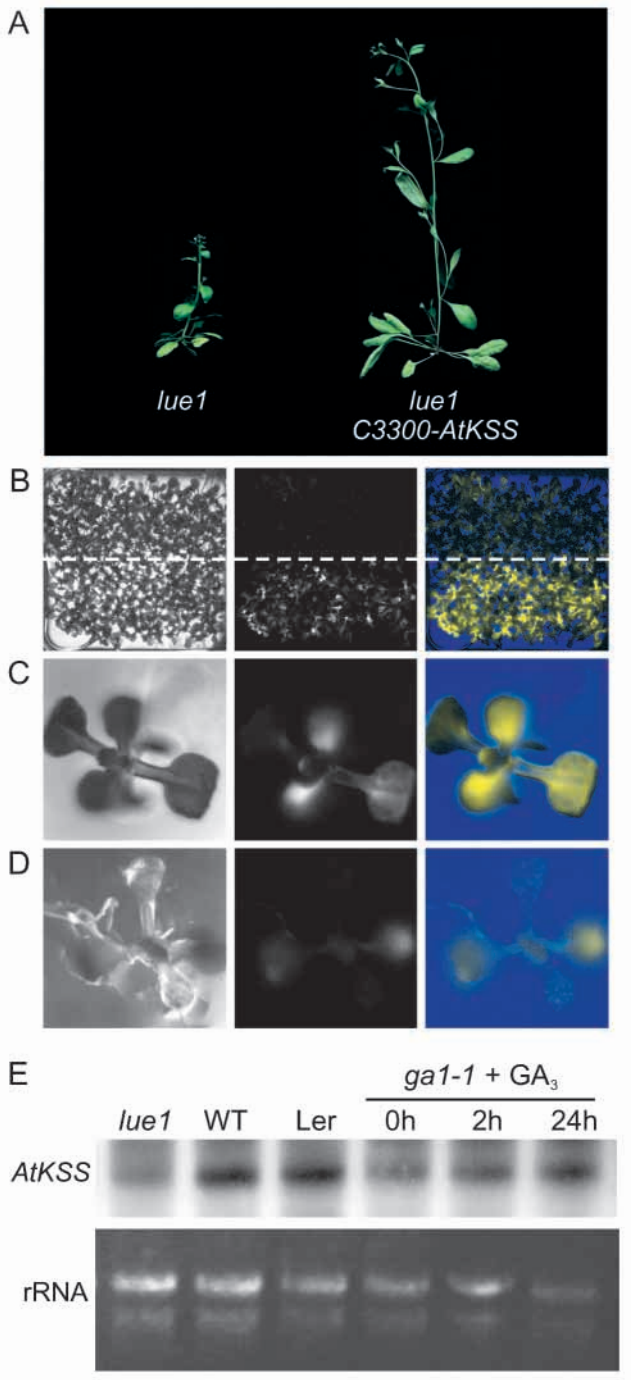


**Fig. 1.** A nonsense mutation in a katanin p60 ortholog gene (*AtKSS*) is responsible for the *lue1* phenotype. (A) Rescue of *lue1* phenotype with the *C3300-AtKSS* transgene. (B) Wild-type (top) and *lue1* (bottom) bioimaging. (C) *lue1* bioimaging. (D) *lue1 C3300-AtKSS* bioimaging. (B-D) Bright field image (left), LUC in vivo image (center), superimposition of bright field and LUC images (right). (E) RNA blot analysis of *AtKSS* mRNA accumulation in *lue1*, wild-type transgenic Col0 (WT), Ler and the GA-deficient *ga1-1* mutant (top). GA treatment (50 μM $GA_3$) was applied to the *ga1-1* mutant for 2 or 24 hours. Ethidium bromide staining of the nitrocellulose membrane after RNA blotting (rRNA, bottom).

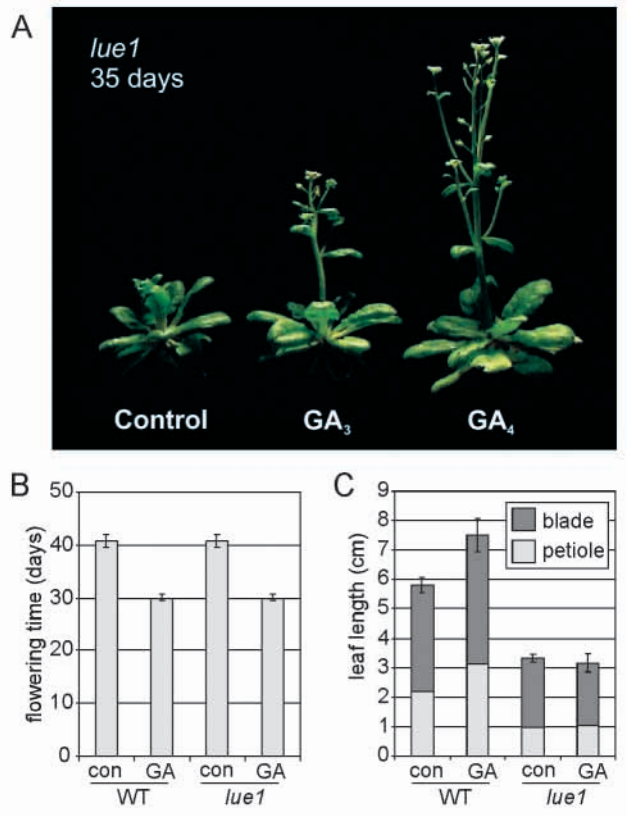


**Fig. 2.** The *lue1* mutant exhibits altered cell elongation in response to GA. (A,B) GA treatment promotes flowering in *lue1*. (A) 35-day-old *lue1* mutants control or sprayed with 10 μM $GA_3$ or $GA_4$ every 4 days. (B) Flowering time of WT and *lue1* plants control or sprayed with 10 μM $GA_3$ every 4 days until bolting. (C) WT and *lue1* leaf elongation upon $GA_3$ treatment. Petiole and blade measurements were performed on adult plants by selecting the longest leaf of control or $GA_3$-treated WT and *lue1* plants (*n* minimum=30).

nutrient medium (Smalle et al., 1997). As expected, hypocotyl growth was enhanced in WT seedlings grown in the presence of ACC (Fig. 3F). Similarly, *lue1* hypocotyl growth was also induced, although apparently to a lesser extent. Both WT and *lue1* root elongations were strongly reduced in the presence of ACC (Fig. 3G). Taken together, these results indicate that although *lue1* is generally responsive to ET, the mutant exhibits inappropriate responses leading to cell growth orientation.

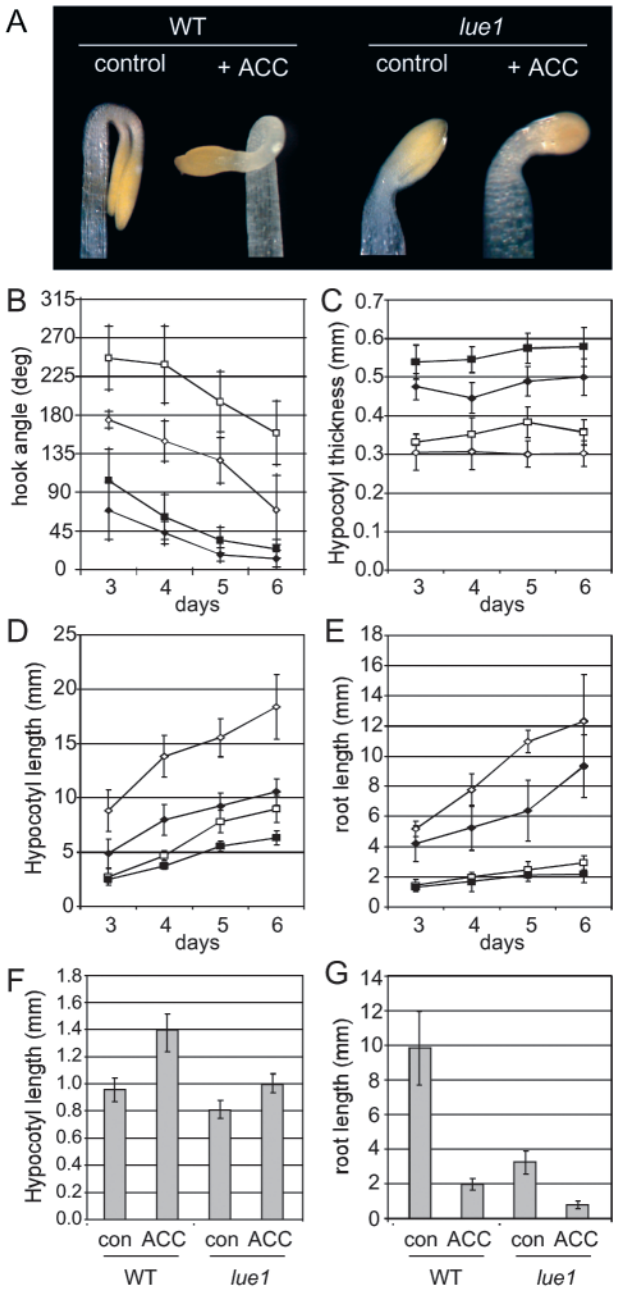


**Fig. 3.** *Lue1* responses to ACC application are partially compromised. (A-E) Seedlings were grown in the dark on MS plates with or without 50 μM ACC. (A) 3-day-old WT and *lue1* seedlings. Hook angle (B), hypocotyl thickness (C), hypocotyl length (D) and root length (E) of WT and *lue1* seedlings (*n* minimum=40). (B-E) ◇, WT control; □, WT+ACC; ◆, *lue1* control; ■, *lue1*+ACC. (F,G) 4-day-old seedlings grown under light conditions on low nutrient medium plates with or without 50 μM ACC. (F) Hypocotyl length. (G) Root length.

## The *lue1* mutant exhibits abnormal CMF and CMT orientation

Before cloning the *AtKSS* gene, the general isotropic cell growth observed in *lue1* led us to investigate CMF and CMT orientation in the mutant. CMF orientation was measured in WT and *lue1* hypocotyls by polarizing microscopy, which is based on the birefringence of CMF (Frey-Wyssling, 1959). Fig. 4A shows an example of polarizing microscopy of WT and *lue1* pitted vessel cells. For WT, the minimum and maximum birefringences were obtained for a rotation angle close to 0° and 45°, respectively. This indicated an average transverse orientation of CMF compared to the main growth axis. By contrast, the minimum and maximum birefringent angles in *lue1* were approximately 45° and 0°, indicating that CMF have an average orientation approaching 45°. Moreover, the generally lower intensity at maximum birefringence is interpreted as a more random orientation in the mutant cells, since staining of the wall showed no difference in wall thickness. Similar polarizing acquisitions were performed on xylem parenchyma, sclerenchyme and epidermal radial walls. Interestingly, most cell types exhibited deviations of CMF in *lue1* compared with WT (Fig. 4B). Moreover, CMF orientation was more variable in *lue1* than in WT cells, as clearly show in the standard deviations of measurements for pitted vessels. A Mann-Whitney rank sum test was performed to test whether the difference in median values of CMF orientation in WT and *lue1* cells was statistically significant. This test confirmed the more random distribution of CMF in *lue1* ($P<0.001$). These results have recently been confirmed and extended by microscopic analyses showing that the aberrant MT orientation caused by the *fra2* mutation in *At*KSS results in distorted deposition of cellulose microfibrils (Burk and Ye, 2002).

As it is generally thought that a CMT network orients the CMF cellulose polymers laid down just outside the plasmalemma, the altered CMF orientation in *lue1* might reflect disorganized CMT. We therefore compared CMT network organization in *lue1* and WT by crossing *lue1* with transgenic plants expressing a translational fusion between GFP and the MT-associated protein4 [MP4 (Marc et al., 1998)]. This reporter fusion decorates CMT in *Arabidopsis* cells without interfering with cytoskeletal organization (Mathur and Chua, 2000). Confocal microscopy revealed a striking difference between WT and *lue1* CMT in interphase cells. CMT in WT cells appeared ordered in transverse arrays, whereas the decorated CMT in *lue1* exhibited a more random distribution (compare Fig. 4C with D). This result is in agreement with previous observations performed on *bot1-5* and *fra2* mutants cells (Bichet et al., 2001; Burk et al., 2001). These observations were confirmed for most cell types investigated, including those of the root, hypocotyl and cotyledon. However, no obvious difference between WT and *lue1* CMT organization was detected in stomata (compare Fig. 4E with F), although *lue1* stomata exhibited a reduced length, comparable to other cell types, when compared to WT. These results suggest that the role of AtKSS in stomatal cell differentiation and development is less pronounced than in other cell types.

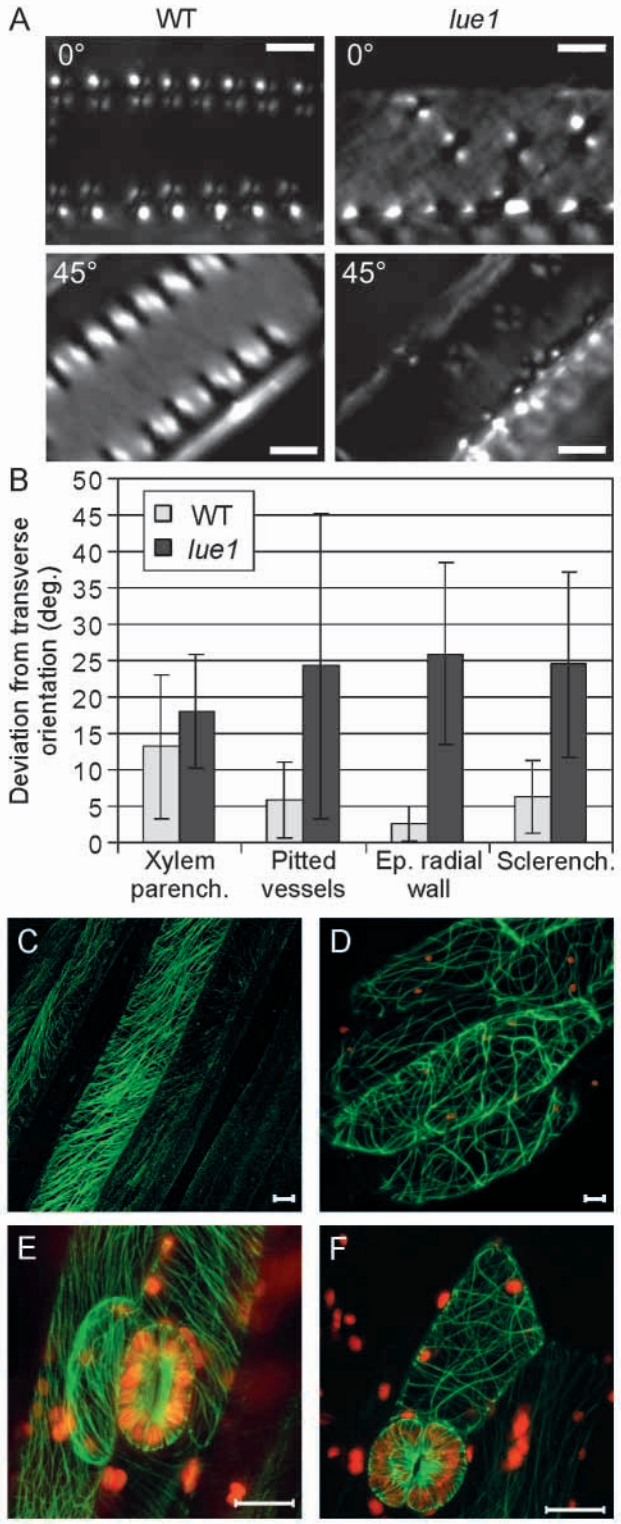


**Fig. 4.** *Lue1* exhibits disorganized CMF and CMT. (A,B) Polarizing microscopy of WT and *lue1* CMF orientation in different cell types. (A) CMF orientation in single pitted vessel cells of WT and *lue1* showing maximum birefringence for rotation angles relative to main growth axis of 45° and 0°, respectively. This indicates a transverse orientation of CMF compared with the main growth axis in WT, whereas the average CMF orientation in *lue1* is 45°. Bars represent 5 μm. (B) Deviation from transverse orientation of CMF in WT and *lue1* cells (*n* minimum=20). (C-F) Confocal microscopy of CMT organization in WT and *lue1* cells. Bars represent 10 μm. The microtubule-decorating GFP-MAP4 reporter was introduced in *lue1* by crossing and CMT organization assessed in segregating $F_2$ seedlings. WT epidermal root (C) and stomata (E) cells. *Lue1* epidermal root (D) and stomata (F) cells.

## The AtKSS protein decorates the CMT

To investigate the subcellular localization of AtKSS and its possible interaction with CMT, we generated transgenic *Arabidopsis* Col0 plants expressing a translational fusion between *AtKSS* and the *GFP* and *GUS* reporters (AtKSS-G-G; Fig. 5A). Interestingly, all herbicide-resistant transgenic plants expressing detectable levels of the GUS and GFP reporters phenocopied *lue1* (Fig. 5B). These plants had the characteristic shorter and thicker organs of *lue1*, including leaves, flowers and siliques. Leaf trichomes were also mainly two branched and frequently distorted. By contrast, all herbicide-resistant transgenic plants that appeared to be wildtype had very weak GUS activities and no detectable GFP (data not shown). Confocal microscopy performed on intact tissue showed that the AtKSS-G-G protein fusion is targeted to the cytoplasm in epidermis root cells (Fig. 5D,E). No GFP was detected in organelles, vacuoles or nuclei. In root cells close to the root tip, no obvious pattern was observed, and GFP appeared as a blurry signal staining the entire cytoplasm. However, in epidermal root cells that were distant from the tip the GFP signal appeared associated with CMT (Fig. 5F,G). Similar CMT labeling by AtKSS-G-G was found in the hypocotyl (Fig. 5H), in the transition zone between root and hypocotyl (Fig. 5I,J) and in stomata (Fig. 5K). Closer examination revealed that GFP decorated CMT bundles while establishing apparent protein aggregations along its fibers (Fig. 5J). This punctate pattern of CMT labeling was particularly prominent in cells close to the transition zone between the root and hypocotyl.

## AtKSS interacts with other MT-related proteins

The connection between AtKSS, CMT organization and GA prompted us to search for proteins that interact with AtKSS. A yeast two-hybrid screen was therefore performed with full-length AtKSS fused to the GAL4-DNA-binding domain (GAL4-BD) as bait. An *Arabidopsis* cv Col0 cDNA library from mature leaves was screened and resulted in the isolation of some 1000 clones, some of which were further characterized (Fig. 6A). Protein-protein interactions in yeast were confirmed by transforming the PJ69-4A strain (auxotrophic for TRP, LEU, HIS and ADE) with plasmids containing GAL4-BD-*AtKSS* (*pGBT7-AtKSS*; TRP marker) and GAL4-activation domain (*pGAD10-prey*; LEU marker). All transformants grew on SD medium lacking TRP, LEU, ADE and HIS (Fig. 6B, right). Additionally, they exhibited strong β-galactosidase activities (Fig. 6B, center). This indicates that the *ADE2* and *HIS3* genes, whose transcriptional control is dependent on GAL4-AD and GAL4-BD interaction, are expressed. By contrast, strains carrying empty *pGBT7* lacking *AtKSS* and the *pGAD10-prey* plasmids exhibited neither auxotrophic growth on medium lacking the nutritional markers (Fig. 6C, right) nor β-galactosidase activities (Fig. 6C, center), confirming the interactions between AtKSS and prey proteins.

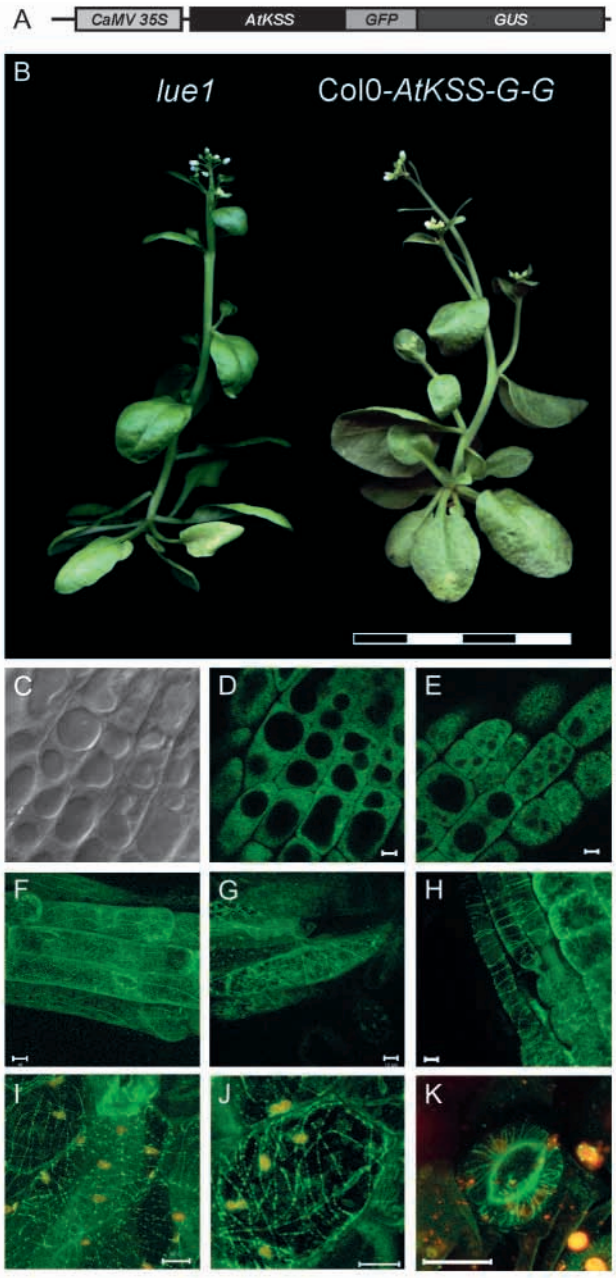


**Fig. 5.** The AtKSS-GFP-GUS protein fusion decorates CMT. (A) Schematic representation of the *CaMV35S-AtKSS-GFP-GUS* reporter construct introduced into *Arabidopsis*. (B) Ectopic expression of the AtKSS-GFP-GUS (AtKSS-G-G) protein fusion in *Arabidopsis* Col0 ecotype phenocopies the *lue1* phenotype. (C) Differential interference contrast (DIC) reference images of D. (D-K) Confocal microscopy of AtKSS-G-G subcellular distribution. GFP fluorescence is encoded in the green channel. Bars represent 10 μm. (D,E) Root epidermis cells close to the root tip. (F,G) Root epidermis cells distal from tip. (H) Hypocotyl. (I,J) Transition zone between root and hypocotyl. (K) Stomata.

A katanin p80 subunit ortholog (Chromosome 1, BAC F11P17) was abundantly represented in the clones obtained from the library screen. Two different clones were obtained encoding the C-terminal domain of this protein, referred to here as KTN-p80.1 (accession number: AAB71474; Fig. 6A). This result is in agreement with previous observations that the C-terminal region of katanin p80 is required for interaction with the katanin p60 subunit in animal cells (Hartman et al., 1998; McNally et al., 2000). Co-immunoprecipitation assays confirmed the interaction between AtKSS and KTN-p80.1 in vitro (Fig. 6D). Database homology searches revealed the presence of three other *Arabidopsis KTN-p80.1*-related genes that are represented in EST databases. Although some of these predicted proteins exhibit low homology with the central region of KTN-p80.1, all share high similarities within their N-terminal WD40 repeats and within the C-terminal region of KTN-p80.1 and katanin p80 subunits from other organisms (Fig. 6E).

Another putative AtKSS-interacting protein (accession number, CAB89396; referred to here as KSN1) was isolated as two independent yeast clones from the library screen. KSN1 contains an ATP/GTP-binding site motif A (P-loop; residues 223-230) and a kinesin motor domain signature (residues 356-367). KSN1 was previously characterized as a cdc2a-interacting peptide [accession number: AJ001729 (de Veylder et al., 1997)]. The *KSN1* cDNA (clone 1.52) isolated in the two-hybrid screen spans residues 473-867, a region with significant similarities to another *Arabidopsis* protein represented by an EST (AB011479.1). Co-immunoprecipitation assays confirmed the interaction between AtKSS and the KSN1 peptide encoded by clone 1.52 (Fig. 6D).

## Discussion

It is well documented that external stimuli and hormones control MT dynamics, but less is known about the molecular mechanisms involved in such control. Here we show that the katanin p60 *Arabidopsis* protein AtKSS plays a role in CMT organization by genetic and cytological analyses of the *lue1* mutant (Meier et al., 2001). This approach indicates that aspects of *At*KSS function may be mediated by GA, in keeping with previous work on MT organization in GA-deficient mutants and other plants (Wenzel et al., 2000; Baluska et al., 1993; Inada and Shimmen, 2000) and that some form of feedback interaction results in effects on expression of GA biosynthetic genes. For example, complementation of *lue1* with the wild-type *AtKSS* gene rescued the mutant phenotype and restored normal expression levels of the *GA5-LUC* reporter transgene in the mutant background. Moreover, progeny of a cross between *lue1* and *bot1-5* (Bichet et al., 2001) exhibited both the dwarf stature and high *GA5-LUC* reporter phenotypes. This indicates that *lue1* and *bot1* are allelic and confirms that the *GA5-LUC* reporter is overexpressed in mutants lacking a functional *AtKSS* gene. These results suggest that MT function and/or AtKSS activity may be involved in feedback modulation of GA biosynthesis via the expression of *AtGA20ox1* and perhaps of *At3ox1* (Meier et al., 2001). An additional link between MT function and GA is suggested by the increase in *AtKSS* mRNA levels in the GA-deficient mutant *ga1-1* following GA application.

An explanation for these effects is that GA affects a distinct signaling pathway that monitors and modulates cell growth. In this model, GA affects cell elongation that induces *AtKSS* and/or represses *AtGA20ox1* indirectly via another pathway. Alternatively, GA and other growth signaling pathways may crosstalk, in which case shared or interacting components exist.

Numerous reports have shown that GA signaling regulates the transcription of target genes and the post-translational control of certain proteins. For example, levels of the *Arabidopsis* GA signaling repressor RGA, a member of the GRAS protein family thought to act as transcription factors (Richards et al., 2000), are rapidly reduced upon GA application (Silverstone

A

| Yeast clone / Size (aa) | Nb. of clones | Homology / Function | Accession number |
|---|---|---|---|
| 1.25 (218) | 12 | KATANIN p80 | AC002294 |
| 1.38 (324) | 10 | KATANIN p80 | AC002294 |
| 1.52 (394) | 2 | KINESIN | AL353995 |
| 1.86 (217) | 1 | Unknown | AC004683 |

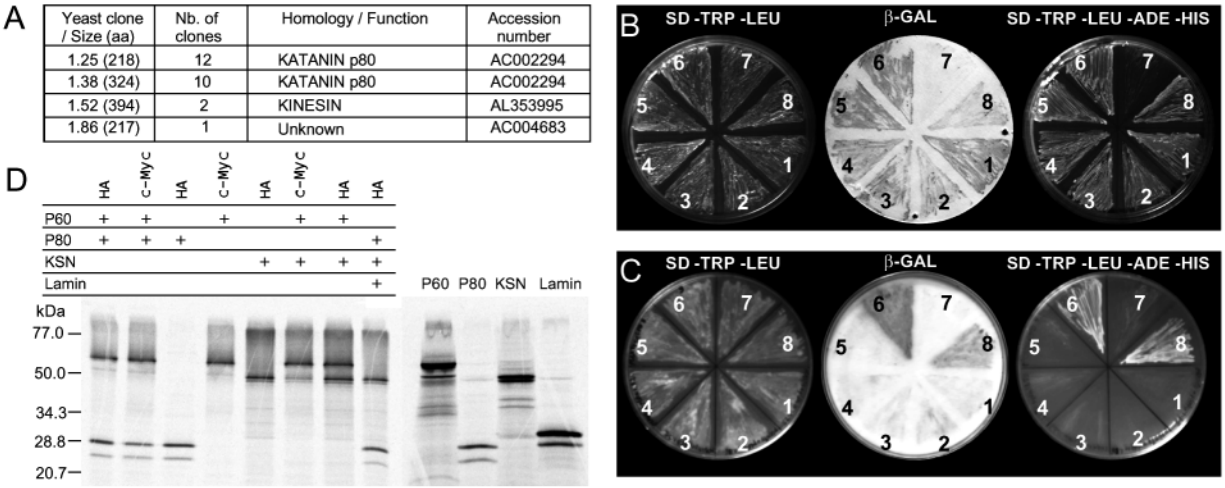


E

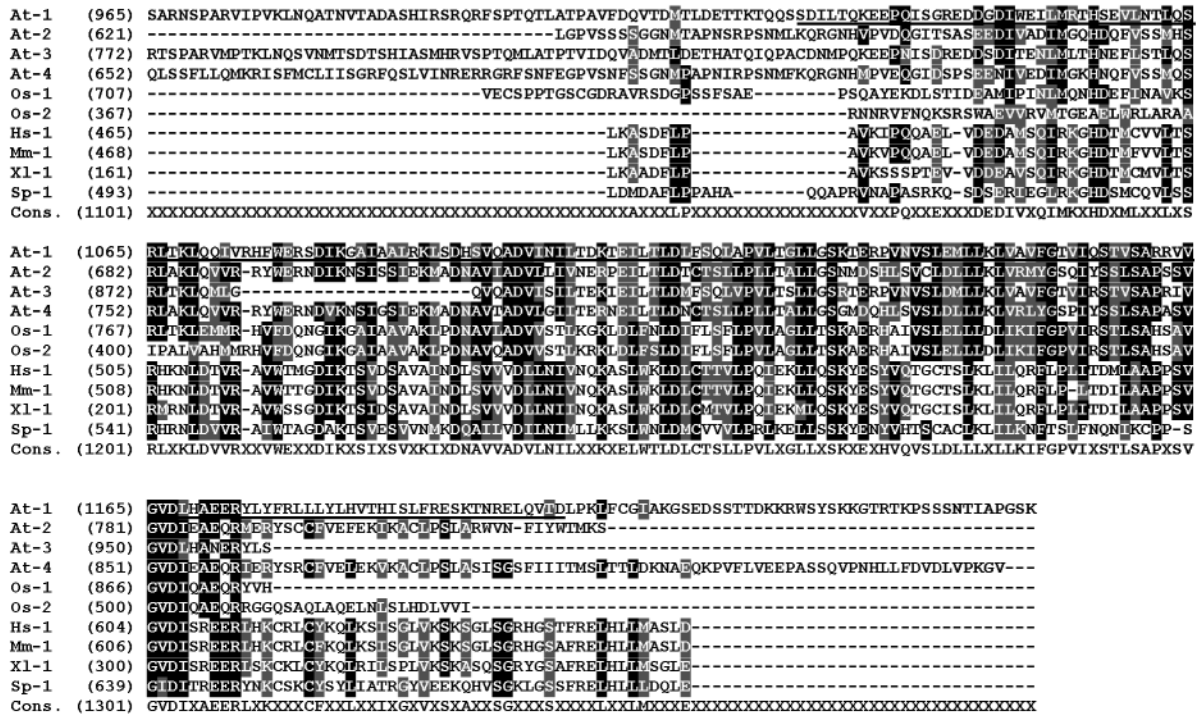


**Fig. 6.** AtKSS protein interactions. (A) Prey proteins isolated from the yeast two-hybrid screen. (B,C) Yeast two-hybrid interactions. Growth of strains on minimal SD media lacking tryptophan (TRP) and leucine (LEU) (left). β-galactosidase assay of a replica of the left panels (center). Growth of yeast strains on minimal SD media lacking TRP, LEU, adenine (ADE) and histidine (HIS) (right). (B) Fusion proteins expressed from the DNA-binding (BD) and activation (AD) domains: 1 (BD: AtKSS; AD: 1.38); 2 (BD: AtKSS; AD: 1.25); 3 (BD: AtKSS; AD: 1.25B2); 4 (BD: AtKSS; AD: KSN1); 5 (BD: AtKSS; AD: 1.86); 6 and 8 (positive controls, Clontech); 7 (negative control, Clontech). (C) Protein-protein interaction assays using empty BD vectors. Yeast strains 1 to 5 had the AD as in B but carried the empty pGBDT7 BD vector. Yeast strains 6 to 8 were as in B. (D) Co-immunoprecipitation of AtKSS and prey proteins (left panel) using in vitro methionine $^{35}$S-labelled translated proteins (right panel). Proteins were incubated in the presence of either anti-HA or anti-c-Myc antibodies. Protein complexes were pulled down using protein-G-coupled Dynabeads. Polypeptides for in vitro translation were: AtKSS (p60): PGABKT7-AtKSS; KTN p80.1 (p80): clone pGADT7-1.25B2; KSN1: clone pGADT7-1.52; LAMIN C: pGBKT7-Lam (Clontech). (E) Sequence alignment of the C-terminal regions of putative katanin p80 proteins. Amino acids residues conserved in at least five sequences are in black boxes, similar residues are in gray. At-1 to At-4, *Arabidopsis* AAB71474, CAC08339, AAD49999 and BAB09559. Os-1 and Os-2, rice BAB63574 and BAB91860. Hs-1, human XP_048046. Mm, mouse BAB26884. Xl-1, *Xenopus laevis* AAC25113. Sp-1, *Strongylocentrotus purpuratus* AAC09329. The consensus (cons.) is presented beneath the alignment. The underlined sequence represents the polypeptide encoded by clone 1.25B2.

et al., 2001). In addition, *SPY* encodes an *O*-linked *N*-acetylglucosamine transferase (OGT) whose loss-of-function produces a constitutive GA-response mutant phenotype (Thornton et al., 1999). OGT addition of *O*-linked *N*-acetylglucosamine may regulate the activity of substrate proteins antagonistically to their modification by phosphorylation (Wells et al., 2001). Possible models of GA action therefore include the direct modification and resultant stabilization of RGA by SPY (Harberd et al., 1998) that is somehow counteracted by GA to derepress the expression of RGA downstream targets, potentially including AtKSS. This model does not, however, explain the effect that loss of *At*KSS function has on the increase in expression of the GA biosynthetic genes *AtGA20ox1* and *At3ox1*, whose expression is normally repressed by GA (Meier et al., 2001). This effect suggests that *At*KSS and/or other MT-associated proteins indirectly affect GA feedback via regulatory pathways to integrate cytoskeletal organization and cell elongation. Although such pathways remain obscure, they may include signaling pathways related to brassinosteroids that also affect MT organization (Catterou et al., 2001) and that we have shown to increase the expression of *AtGA20ox1* (Bouquin et al., 2001).

The ectopic expression of a fusion reporter between AtKSS, GFP and GUS in wild-type Col0 plants resulted in a dwarf phenotype similar to that of *lue1*. This suggests that the AtKSS-G-G fusion functions as a dominant negative form of AtKSS that lacks all or some of its activity. This hypothesis is in agreement with the fact that the AtKSS-G-G reporter fusion failed to rescue the *lue1* mutant (data not shown). However, since AtKSS-G-G decorates CMT, this reporter fusion is apparently correctly targeted and may compete with endogenous AtKSS protein for factors important for its function. If both the MT-interacting and katanin p80-interacting domains are functional in AtKSS-G-G, then the C-terminal ATPase domain required for MT-severing activity (Hartman and Vale, 1999) may not be fully functional in the fusion. Such a model is consistent with the fact that both the *lue1* and *fra2* mutations occur in the ATPase domain of AtKSS. In addition, we show that *AtKSS* mRNA levels are detectable in *lue1*, although at significantly lower levels than in WT. This suggests that the *lue1* phenotype is primarily the result of an inactive katanin p60 rather than a lack of the protein. We note that the fusion between the two reporters and AtKSS was designed in the AtKSS C-terminus to avoid disturbing its N-terminal, MT-interacting domain or potential post-translational processing including glycosylation.

In all our observations, the AtKSS-G-G reporter was confined to the cytoplasm. More specifically, the protein was observed as a blurry signal in epidermal cells close to the root tip, whereas distinct CMT labeling patterns were detected in other cells such as in the transition zone between the root and hypocotyl, the hypocotyl and stomata. We also observed phragmoplast labeling by AtKSS-G-G, although the signal intensity appeared weaker and more random than in interphase cells (data not shown). Since mitosis and cytokinesis were apparently unaffected in the allelic *bot1-5* and *fra2* mutants (Bichet et al., 2001; Burk et al., 2001), these results indicate that the role of AtKSS in modulating MT dynamics is less marked during mitosis than during interphase. This may be due to a difference in protein targeting, although we cannot exclude transcriptional control of *AtKSS*. Recently the *Caenorhabditis elegans* Nedd8 ubiquitin-like protein modification pathway that regulates cell cycle progression was shown to negatively regulate katanin, thus allowing the formation of the mitotic spindle (Kurz et al., 2002). It is therefore possible that the *Arabidopsis* katanin is similarly targeted for ubiquitin-mediated degradation when assembly of the mitotic spindle is required.

In interphase cells, CMT labeling by the AtKSS-G-G reporter frequently appeared as a punctate pattern, suggesting that the reporter fusion aggregates along the CMT. Interestingly, *C. elegans* katanin p60 forms hexameric rings around MT (Hartman et al., 1998; Hartman and Vale, 1999). It is therefore likely that the AtKSS-G-G structures observed along the CMT correspond to aggregations of katanin rings. This would imply that the AtKSS-G-G ATPase domain binds ATP because katanin p60 oligomerization is an ATP-dependent process (Hartman and Vale, 1999). However, the presence of intact but mis-oriented CMT in plants expressing AtKSS-G-G suggests that this fusion may have reduced or no ATPase activity required for MT severing. For example, overexpression of human katanin p60 in HeLa cells results in disassembly of the interphase MT cytoskeleton (McNally et al., 2000), which is clearly not the case in plant cells that overexpress AtKSS-G-G. The importance of ATPase activity in vivo could be addressed with reporters based on GFP fused to the AtKSS N-terminus or on AtKSS forms mutated to block nucleotide hydrolysis and trap the enzyme in the ATP-bound state (Hartman and Vale, 1999).

Preliminary time-course observations of GFP-MAP4 reporter fluorescence indicated that wild-type CMT undergo rapid shrinkage and reorientation within minutes of transfer of seedlings from dark to light (data not shown). By contrast, modifications of the CMT network appeared to be slower in *lue1*. It is therefore probable that the abnormal CMT organization reflects the inability of *lue1* CMT to respond rapidly to stimuli normally responsible for CMT reorientation and anisotropic cell growth. This would lead to the abnormal deposition of CMF in *lue1* and contribute to the general organ fragility observed in *fra2*, *bot1-5* and *lue1*, as well as their apparent insensitivity to hormone-mediated cell elongation.

A yeast two-hybrid screen with AtKSS as bait identified a katanin p80 subunit ortholog (KTN-p80.1) as an *At*KSS interaction partner. This result confirms that *At*KSS has a katanin-like function. The two KTN-p80.1 clones isolated (1.38 and 1.25) encode the C-terminus and implicate this region in the interaction with the katanin p60. More specifically, clone 1.25 encodes the last 222 residues of KTN-p80.1, including 101 amino acids conserved among katanin p80-like proteins. This domain is therefore sufficient to establish interactions between katanin heterodimers, as shown in directed yeast two-hybrid and co-immunoprecipitation assays using a truncated version (1.25B2) of clone 1.25. Sequence homology searches identified three other *KTN-p80.1*-related *Arabidopsis* genes with strong homology to other katanin p80s, particularly in the N-terminal WD40 repeats and in the C-terminal katanin-p60-interacting region. Since they are all represented in EST databases, it is surprising that only KTN-p80.1 was isolated in the two-hybrid screen. It may be that the other KTN-p80-encoding clones were under-represented in the cDNA library, and we therefore cannot

exclude the possibility that AtKSS interacts with other KTN-p80.1-like proteins in planta. In animal cells, the katanin p80 subunit targets the katanin complex to centrosomes and regulates the MT-severing activity of the p60 subunit (Hartman et al., 1998; McNally et al., 2000). Database searches indicated that *Arabidopsis* has only one copy of AtKSS. However, several homologous proteins harboring the AAA ATPase domain, but lacking the N-terminal region that contains the MT- and katanin-p80-interacting domains, are present in *Arabidopsis*. Moreover, the genetic isolation of null mutant alleles of *AtKSS* suggests that there are no other genes with completely redundant functions. Therefore, the involvement of AtKSS in multiple and distinct MT-related activities may require tight control of its subcellular targeting. The fact that all katanin-P80-related proteins from *Arabidopsis* are highly similar within the WD40 domains and katanin-p60-interacting C-terminal regions, but otherwise exhibit low homologies in the central regions, suggests that the central region may be involved in differential targeting of the katanin heterodimers. For example, KTN p80.1 could target AtKSS to CMT, whereas another p80 form could target it to the phragmoplasm. This would explain why the other katanin p80s may be under-represented in the yeast two-hybrid library because there are less cells undergoing division than cells in interphase. GUS reporter fusions using various katanin p80 promoters may address this question. However, the fact that loss-of-function alleles of *AtKSS* are apparently not impaired in cytokinesis and mitosis indicates that this katanin p60 subunit plays a minor role in these cellular events. Katanin activity analogous to that required in the spindle pole of animal cells undergoing cell division may therefore be supplied by other MT-severing proteins in plant cells.

Another AtKSS-interacting protein identified here (KSN1) harbors an ATP/GTP-binding site motif A (P-loop) and a kinesin motor domain signature, although these regions were apparently not involved in the interaction with AtKSS. Kinesin motor enzymes hydrolyze ATP to generate force and movement along MT. Numerous studies have shown a role for kinesins in MT-associated activities such as vesicle transport along MT, mitosis and meiosis. Homology searches indicated that KSN1 is member of a small family that includes another protein exhibiting 77% identity with KSN1 (AB011479.1). An A-type cyclin-dependent kinase (CDK) designated Cdc2 was previously shown to interact with a KSN1 peptide (de Veylder et al., 1997). Interestingly, Cdc2 cosedimented with taxol-stabilized MT (Weingartner et al., 2001). Additionally, a functional Cdc2-GFP fusion decorated the anaphase spindle and phragmoplast. Subcellular localization of the Cdc2-GFP fusion was shown to be cell-cycle-dependent and tightly associated with the nucleus during interphase. Taken together with our inability to detect the AtKSS-G-G fusion in the nucleus, the association of AtKSS with KSN1 and Cdc2, if any, is likely to take place during mitosis. Alternatively, AtKSS and Cdc2a could compete for recruitment of KSN1, although we found no significant sequence homologies between AtKSS and Cdc2 to indicate conserved binding regions. Interestingly, immunological experiments with antibodies targeted either against the C-terminal region of Cdc2 or the PSTAIRE motif in the cyclin-binding domain found in A-type CDKs showed that Cdc2 was associated with CMT from various plants (Hemsley et al., 2001). This suggests that a multimeric protein complex including katanin heterodimers KSN1 and Cdc2a could be involved in CMT processing.

The growing number of MT-associated proteins (MAP) and MT regulatory proteins that are being characterized in plants is rapidly increasing our understanding of MT genesis and dynamics. Among these MAPs, AtKSS seems to play a central role, especially in the integration of hormonal signals that lead to anisotropic cell growth by severing CMT, allowing reorientation of MT growth and thus CMF deposition. Further work is required to elucidate the molecular mechanisms that lead to the transcriptional regulation of GA biosynthetic genes and the exact involvement of AtKSS in mitosis and cytokinesis.

We are grateful to Janni Kristensen for technical assistance. This research was funded by the European Union (grant number CT96–0062 and CT96–0621 to J.M.). T.B. was funded by a postdoctoral Marie Curie Research training grant.

## References

**Arioli, T., Peng, L., Betzner, A. S., Burn, J., Wittke, W., Herth, W., Camilleri, C., Hofte, H., Plazinski, J., Birch, R. et al.** (1998). Molecular analysis of cellulose biosynthesis in *Arabidopsis*. *Science* **279**, 717-720.

**Azimzadeh, J., Traas, J. and Pastuglia, M.** (2001). Molecular aspects of microtubule dynamics in plants. *Curr. Opin. Plant Biol.* **4**, 513-519.

**Baluska, F., Parker, J. S. and Barlow, P. W.** (1993). A role for gibberellic acid in orienting microtubules and regulating cell growth polarity in the maize root cortex. *Planta* **191**, 149-157.

**Bechtold, N. and Pelletier, G.** (1998). In planta Agrobacterium-mediated transformation of adult *Arabidopsis thaliana* plants by vacuum infiltration. *Methods Mol. Biol.* **82**, 259-266.

**Bell, C. J. and Ecker, J. R.** (1994). Assignment of 30 microsatellite loci to the linkage map of *Arabidopsis*. *Genomics* **19**, 137-144.

**Bichet, A., Desnos, T., Turner, S., Grandjean, O. and Hofte, H.** (2001). BOTERO1 is required for normal orientation of cortical microtubules and anisotropic cell expansion in *Arabidopsis*. *Plant J.* **25**, 137-148.

**Bouquin, T., Meier, C., Foster, R., Nielsen, M. E. and Mundy, J.** (2001). Control of specific gene expression by gibberellin and brassinosteroid. *Plant Physiol.* **127**, 450-458.

**Burk, D. H. and Ye, Z.-H.** (2002). Alteration of oriented deposition of cellulose microfibrils by mutation of a katanin-like microtubule-severing protein. *Plant Cell* **14**, 1-17.

**Burk, D. H., Liu, B., Zhong, R., Morrison, W. H. and Ye, Z. H.** (2001). A katanin-like protein regulates normal cell wall biosynthesis and cell elongation. *Plant Cell* **13**, 807-827.

**Catterou, M., Dubois, F., Schaller, H., Aubanelle, L., Vilcot, B., Sangwan-Norreel, B. S. and Sangwan, R. S.** (2001). Brassinosteroids, microtubules and cell elongation in *Arabidopsis thaliana*. II. Effects of brassinosteroids on microtubules and cell elongation in the bul1 mutant. *Planta* **212**, 673-683.

**de Veylder, L., Segers, G., Glab, N., van Montagu, M. and Inze, D.** (1997). Identification of proteins interacting with the *Arabidopsis* Cdc2aAt protein. *J. Exp. Bot.* **48**, 2111-2112.

**Frey-Wyssling, A.** (1959). *Die Pflanzliche Zellwand*. Springer-Verlag, Berlin-Göttingen-Heidelberg.

**Harberd, N. P., King, K. E., Carol, P., Cowling, R. J., Peng, J. and Richards, D. E.** (1998). Gibberellin: inhibitor of an inhibitor of…? *BioEssays* **20**, 1001-1008.

**Hartman, J. J., Mahr, J., McNally, K., Okawa, K., Iwamatsu, A., Thomas, S., Cheesman, S., Heuser, J., Vale, R. D. and McNally, F. J.** (1998). Katanin, a microtubule-severing protein, is a novel AAA ATPase that targets to the centrosome using a WD40-containing subunit. *Cell* **93**, 227-287.

**Hartman, J. J. and Vale, R. D.** (1999). Microtubule disassembly by ATP-dependant oligomerization of the AAA enzyme katanin. *Science* **286**, 782-785.

**Hemsley, R., McCutcheon, S., Doonan, J. and Lloyd, C.** (2001). P34cdc2 kinase is associated with cortical microtubules from higher plant protoplasts. *FEBS Lett.* **508**, 157-161.

**Inada, S. and Shimmen, T.** (2000). Regulation of elongation growth by gibberellin in root segments of Lemma minor. *Plant Cell Physiol.* **41**, 932-939.

**Ishida, K. and Katsumi, M.** (1992). Effect of gibberellin and abscissic acid on the cortical microtubule orientation in hypocotyl cells of light-grown cucumber seedlings. *Int. J. Plant Sci.* **153**, 155-163.

**Koornneef, M. and van der Veen, J. H.** (1980). Induction and analysis of gibberellin sensitive mutants in *Arabidopsis thaliana* (L.) Heynh. *Theor. Appl. Genet.* **58**, 257-263.

**Kost, B., Spielhofer, P. and Chua, N.-H.** (1998). A GFP-mouse talin fusion protein labels plant actin filaments in vivo and visualizes the actin cytoskeleton in growing pollen tubes. *Plant J.* **16**, 393-401.

**Kost, B., Mathur, J. and Chua, N.-H.** (1999). Cytoskeleton in plant development. *Curr. Opin. Plant Biol.* **2**, 462-472.

**Kurz, T., Pintard, L., Willis, J. H., Hamill, D. R., Gonczy, P., Peter, M. and Bowerman, B.** (2002). Cytoskeletal regulation by the Nedd8 ubiquitin-like protein modification pathway. *Science* **295**, 1294-1298.

**Marc, J., Granger, C. L., Brincat, J., Fisher, D. D., Kao, T., McCubbin, A. G. and Cyr, R. J.** (1998). A GFP-MAP4 reporter gene for visualizing cortical microtubule rearrangements in living epidermal cells. *Plant Cell* **10**, 1927-1940.

**Mathur, J. and Chua, N.-H.** (2000). Microtubule stabilization leads to growth reorientation in *Arabidopsis trichomes*. *Plant Cell* **12**, 465-477.

**McClinton, R. S., Chandler, J. S. and Callis, J.** (2001). cDNA isolation, characterization, and protein intracellular localization of a katanin-like p60 subunit from *Arabidopsis thaliana*. *Protoplasma* **216**, 181-190.

**McNally, K. P., Bazirgan, O. A. and McNally, F. J.** (2000). Two domains of p80 katanin regulate microtubule severing and spindle pole targeting by p60 katanin. *J. Cell Sci.* **113**, 1623-1633.

**Meier, C., Bouquin, T., Nielsen, M. E., Raventos, D., Mattsson, O., Rocher, A., Schomburg, F., Amasino, R. M. and Mundy, J.** (2001). Gibberellin response mutants identified by luciferase imaging. *Plant J.* **25**, 509-519.

**Nicol, F., His, I., Jaunau, A., Vernhettes, S., Canut, H. and Hofte, H.** (1998). A plasma membrane-bound putative endo-1,4-beta-D-glucanase is required for normal wall assembly and cell elongation in *Arabidopsis*. *EMBO J.* **17**, 5563-5576.

**Richards, D. E., Peng, J. and Harberd, N. P.** (2000). Plant GRAS and metazoan STATs: one family? *BioEssays* **22**, 573-577.

**Shibaoka, H.** (1994). Plant hormone-induced changes in the orientation of cortical microtubules. *Annu. Rev. Plant Physiol. Plant Mol. Biol.* **45**, 527-544.

**Silverstone, A. L., Jung, H. S., Dill, A., Kawaide, H., Kamiya, Y. and Sun, T. P.** (2001). Repressing a repressor: gibberellin-induced rapid reduction of the RGA protein in *Arabidopsis*. *Plant Cell* **13**, 1555-1566.

**Smalle, J., Haegman, M., Kurepa, J., van Montagu, M. and Straeten, D. V.** (1997). Ethylene can stimulate *Arabidopsis* hypocotyl elongation in the light. *Proc. Natl. Acad. Sci. USA* **94**, 2756-2761.

**Stoppin-Mellet, V., Gaillard, J. and Vantard, M.** (2002). Functional evidence for in vitro microtubule severing by the plant katanin homolog. *Biochem. J.* **365**, 337-342.

**Thornton, T. M., Swain, S. M. and Olszewski, N. E.** (1999). Gibberellin signal transduction presents…the SPY who O-GlcNAc'd me. *Trends Plant Sci.* **4**, 424-428.

**Wasteneys, G. O.** (2002). Microtubule organization in the green kingdom: chaos or self-order? *J. Cell Sci.* **115**, 1345-1354.

**Webb, M., Jouannic, S., Foreman, J., Linstead, P. and Dolan, L.** (2002). Cell specification in the *Arabidopsis* root epidermis requires the activity of ECTOPIC ROOT HAIR 3-a katanin-p60 protein. *Development* **129**, 123-131.

**Weingartner, M., Binarova, P., Drykova, D., Schweighofer, A., David, J. P., Heberle-Bors, E., Doonan, J. and Bogre, L.** (2001). Dynamic recruitment of Cdc2 to specific microtubule structures during mitosis. *Plant Cell* **13**, 1929-1943.

**Wells, L., Vosseller, K. and Hart, G. W.** (2001). Glycosylation of nucleocytoplasmic proteins: signal transduction and O-GLcNAc. *Science* **291**, 2376-2378.

**Wenzel, C. L., Williamson, R. E. and Wasteneys, G. O.** (2000) Gibberellin-induced changes in growth anisotropy precede gibberellin-dependent changes in cortical microtubule orientation in developing epidermal cells of barley leaves. Kinematic and cytological studies on a gibberellin-responsive dwarf mutant, M489. *Plant Physiol.* **124**, 813-822.

**Whittington, A. T., Vugrek, O., Wei, K. J., Hasenbein, N. G., Sugimoto, K., Rashbrooke, M. C. and Wasteneys, G. O.** (2001). MOR1 is essential for organizing cortical microtubules in plants. *Nature* **411**, 610-613.

**Zandomeni, K. and Schopfer, P.** (1993). Reorientation of microtubules at the outer epidermal wall of maize coleoptiles by phytochrome, blue light photoreceptor and auxin. *Protoplasma* **173**, 103-112.

**Zandomeni, K. and Schopfer, P.** (1994). Mechanosensory microtubule reorientation in the epidermis of maize coleoptiles subjected to bending stress. *Protoplasma* **182**, 96-101.

**Zuo, J., Niu, Q. W., Nishizawa, N., Wu, Y., Kost, B. and Chua, N.-H.** (2000). KORRIGAN, an *Arabidopsis* endo-1,4-beta-glucanase, localizes to the cell plate by polarized targeting and is essential for cytokinesis. *Plant Cell* **12**, 1137-1152.